Disclaimer: *This is a pre-publication version of the article Wyatt et al. Biogeosciences, 18, 4265–4280, 2021. Readers are recommended to consult the final published version for accuracy and citation at https://doi.org/10.5194/bg-18-4265-2021.*

Seasonal cycling of zinc and cobalt in the Southeast Atlantic along the GEOTRACES GA10 section.

Neil J. Wyatt[1], Angela Milne[2], Eric P. Achterberg[3], Thomas J. Browning[3], Heather A. Bouman[4], E. Malcolm S. Woodward[5], Maeve C. Lohan[1].

[1]Ocean and Earth Science, National Oceanography Centre, University of Southampton, Southampton, United Kingdom.

[2]School of Geography, Earth and Environmental Sciences, University of Plymouth, Plymouth, United Kingdom.

[3]Marine Biogeochemistry Division, GEOMAR Helmholtz Centre for Ocean Research, Kiel, Germany.

[4]Department of Earth Sciences, University of Oxford, Oxford, United Kingdom.

[5]Plymouth Marine Laboratory, Plymouth, United Kingdom.

Correspondence to: N. J. Wyatt (n.j.wyatt@soton.ac.uk)

Abstract

We report the distributions and stoichiometry of dissolved zinc (dZn) and cobalt (dCo) in sub-tropical and sub-Antarctic waters of the Southeast Atlantic Ocean during austral spring 2010 and summer 2011/12. In sub-tropical surface waters, mixed-layer dZn and dCo concentrations during early spring were 1.60 ± 2.58 nM and 30 ± 11 pM, respectively, compared with summer

values of 0.14 ± 0.08 nM and 24 ± 6 pM. The elevated spring dZn concentrations resulted from an apparent offshore transport of elevated dZn at depths between 20 – 55 m, derived from from the Agulhas Bank. In contrast, open-ocean sub-Antarctic surface waters displayed largely consistent inter-seasonal mixed-layer dZn and dCo concentrations of 0.10 ± 0.07 nM and 11 ± 5 pM, respectively. Trace metal stoichiometry, calculated from concentration inventories, suggest a greater overall removal for dZn relative to dCo in the upper water column of the Southeast Atlantic with an inter-seasonally decreasing dZn/dCo inventory ratios of 19 to 5 mol mol^{-1} and 13 to 7 mol mol^{-1} for sub-tropical surface water and sub-Antarctic surface water, respectively. In this paper, we investigate how the seasonal influences of external input and phytoplankton succession may relate to the distribution of dZn and dCo, and variation in dZn/dCo stoichiometry, across these two distinct ecological regimes in the Southeast Atlantic.

1. Introduction

The trace metal micronutrients zinc (Zn) and cobalt (Co) play an important role in the productivity of the oceans as key requirements in marine phytoplankton metabolism (Morel, 2008; Twining and Baines, 2013). Zinc is required for the acquisition of inorganic carbon and organic phosphorus via the carbonic anhydrase and alkaline phosphatase metalloenzymes, respectively (Morel et al., 1994; Shaked et al., 2006; Cox and Saito, 2013). The requirement for Co stems from its obligation in the biosynthesis of vitamin B_{12} (Raux et al., 2000; Rodionov et al., 2003) and, like Zn, its potential roles as a metal cofactor in carbonic anhydrase and alkaline phosphatase (Morel et al., 1994; Jakuba et al., 2008; Saito et al., 2017). Significantly, both dissolved Zn (dZn) and Co (dCo) are often scarce in surface seawater with mean concentrations that are often similar to, or relatively depleted, compared with typical cellular requirements of phytoplankton (Moore et al., 2013; Moore, 2016). Hence, dZn and dCo availability have the potential to regulate phytoplankton metabolism and growth rates in some

ocean regions (Sunda and Huntsman, 1992; Saito et al., 2002; Franck et al., 2003; Shaked et al., 2006; Bertrand et al., 2007; Jakuba et al., 2012; Mahaffey et al., 2014; Chappell et al., 2016; Browning et al., 2017).

The role for Zn and Co in carbonic anhydrase establishes an interaction between their ocean cycles, whereby biochemical substitutions between the enzyme-bound metals enables a stoichiometric plasticity in their cellular requirements that can negate the effect of limited availability. For example, a number of eukaryotic algae can substitute Zn for Co, as well as cadmium (Cd), in carbonic anhydrase when seawater dZn concentrations are low (Price and Morel, 1990; Sunda and Huntsman, 1995; Lane and Morel, 2000; Xu et al., 2007; Saito and Goepfert, 2008; Kellogg et al., 2020). In contrast, the prokaryotic picocyanobacteria *Synechococcus* and *Prochlorococcus* appear to have an absolute Co requirement (Sunda and Huntsman, 1995; Saito et al., 2002; Hawco and Saito, 2018). The availability and stoichiometry of dZn and dCo may therefore also exert a key control on phytoplankton community structure in some ocean regions (Leblanc et al., 2005; Saito et al., 2010; Chappell et al., 2016).

With the arrival of GEOTRACES research cruises, a number of studies have provided comprehensive data on the basin-scale distributions of Zn and Co in the Atlantic Ocean (e.g. Bown et al., 2011; Noble et al., 2012, 2017; Wyatt et al., 2014; Roshan et al., 2015; Middag et al., 2018). Such efforts have transformed our understanding of the biogeochemical processes associated with Zn and Co cycling (Saito et al., 2017; Vance et al., 2017; Weber et al., 2018; Tagliabue et al., 2018; Roshan et al., 2018) yet there are still geographically important regions of the Atlantic that remain largely understudied, including the Southeast Atlantic.

The Sub-Tropical Front (STF) of the Southeast Atlantic represents the convergence of warm, predominately macronutrient-limited Sub-Tropical Surface Water (STSW) and cold, iron-limited but macronutrient enriched sub-Antarctic Surface Water (SASW), creating one of the most dynamic nutrient regimes in the oceans (Ito et al., 2005; Browning et al., 2014; Moore,

2016). Here, the relative supply and availability of macronutrients and iron (Fe) exert an important control in maintaining the elevated phytoplankton stock and productivity that is typical of this frontal region, particularly during austral spring and summer (Moore and Abbott, 2000; Ito et al., 2005; Browning et al., 2014). Dissolved Zn is also depleted in SASW that flows northwards to converge with STSW at the STF (Wyatt et al., 2014). However, the potential role for Zn in the mediation of phytoplankton distribution and community structure in this region is currently unclear.

Using data from two UK-GEOTRACES cruises (transect GA10) this study examines the seasonal availability and ecological stoichiometry of dZn and dCo, by analysis of their relationships with phosphate, in upper ocean waters of the Southeast Atlantic. These data, together with measurements of phytoplankton pigment biomass and community structure, offer an improved knowledge of the seasonal influences of external input and phytoplankton succession on the distribution and cycling of Zn and Co in these dynamic waters.

2. Methods

2.1. Sampling methods

Seawater samples were collected during two UK-GEOTRACES cruises in the South Atlantic Ocean (GA10, Fig. 1). The first cruise (D357) took place during austral spring 2010 (18th October to 22nd November 2010), sampling the Southeast Atlantic on-board the *RSS Discovery*. During D357, two transects were completed between Cape Town and the zero meridian that represent early austral spring (D357-1) and late austral spring (D357-2), respectively. The second cruise (JC068) took place during austral summer 2011/2012 (24th December 2011 to 27th January 2012), along the same transect of the first cruise and continuing along 40ºS between Cape Town and Montevideo, Uruguay, on-board the *RSS James Cook*. For JC068, we present here only the repeat transect data between Cape Town and 13°W that

represents the Southeast Atlantic aspect of this transect. The stations occupied during the three transects were not identical, but rather represent a coverage of the Southern Ocean and sub-tropical waters present. Where stations were reoccupied during one or more transects, they have the same station number.

All sampling bottles were cleaned according to the procedures detailed in the GEOTRACES sample handling protocols (Cutter et al., 2010). Seawater and particulate samples below 15 m depth were collected using a titanium-frame CTD with 24 trace metal clean 10 L Teflon-coated OTE (Ocean Test Equipment) Niskin bottles deployed on a plasma rope. Sub-samples for dissolved trace metal analysis were filtered through 0.8/0.2 µm cartridge filters (AcroPak™ 500, Pall) into 125 mL low density polyethylene bottles inside a class 1000 clean air container. Each sub-sample was acidified to pH 1.7 (0.024 M) by addition of 12 M hydrochloric acid (HCl, UpA, Romil) under a class 100 laminar flow hood. Vertical sampling for dissolved trace metals was augmented by surface samples collected at each station using a towed 'fish' positioned at approximately 3-5 m depth. Fish samples were filtered in-line and acidified as described for samples collected from the titanium sampling system. Particulate samples were collected onto acid clean 25 mm, 0.45 µm, polyethersulfone membrane disc filters (Supor®, Pall) and stored frozen (-20ºC) until shore-based analysis.

2.2. Trace metal analysis

Dissolved Co was determined in the ISO accredited clean room facility (ISO 9001) at the University of Plymouth (UK) using flow injection with chemiluminescence detection, modified from the method of Cannizzaro et al. (1999) as described by Shelley et al. (2010). Briefly, dCo was determined in UV-irradiated samples using the reaction between pyrogallol (1,2,3-trihydrobenzene) and hydrogen peroxide formed in the presence of Co. Standards (20 – 120 pM Co) were prepared in 0.2 µm filtered low-dCo seawater (16.5 ± 5.2 pM, n = 15) by

126 serial dilution of a 1000 ppm Co ICP-MS standard (Romil, UK). The accuracy of the analytical
127 method was validated by quantification of dCo in SAFe (S and D2) and GEOTRACES (GD)
128 reference seawater (Table 1). There was no detectable analytical dCo blank and the limit of
129 detection (3σ of the lowest concentration standard) was 1.98 ± 0.87 pM (n = 15).
130 Dissolved Zn was determined using flow injection coupled with fluorescence detection,
131 modified from the method of Nowicki et al. (1994) and described previously for this
132 GEOTRACES section by Wyatt et al. (2014). The accuracy of the analytical method was
133 validated by quantification of dZn in SAFe (S and D2) reference seawater (Table 1). The blank
134 for dZn FIA was 0.14 ± 0.13 nM and the limit of detection (3σ of the lowest concentration
135 standard) was 0.01 ± 0.01 nM (n = 15).
136 Measurement uncertainties were estimated after the Nordtest approach (Worsfold et al., 2019)
137 where a combined uncertainty (u_c) is computed from day-to-day within-lab reproducibility and
138 uncertainties associated with the determination of reference materials (Table 1). This approach
139 creates higher uncertainties than those previously published for dZn and dCo analyses but
140 provides a more realistic estimation of analytical uncertainty. During this study, the u_c for dZn
141 and dCo analysis was 22 and 19 %, respectively, similar to the 13 – 25 % reported by Rapp et
142 al. (2017) for the determination of trace metals, including dZn and dCo, by on-line pre-
143 concentration and high-resolution sector field ICP-MS detection. The elevated u_c within our
144 data results from the greater uncertainty surrounding the very low dZn and dCo concentration
145 SAFe S reference sample whereas the dZn and dCo u_c using only the Safe D2 are <5 %.
146 Hereafter, when presenting low dZn and dCo concentrations for comparison with
147 phytoplankton biological requirements (Section 3.5), we apply a fixed u_c of 20 % to our data.
148 Total particulate trace metals (i.e. pZn, pCo, pTi) were determined using inductively coupled
149 plasma-mass spectrometry (Thermo Fisher XSeries-2) following a sequential acid digestion
150 modified from Ohnemus et al. (2014). Potential interferences (e.g. $_{40}Ar_{16}O$ on $_{56}Fe$) were

minimized through the use of a collision/reaction cell utilizing 7 % H in He and evaluation of efficiency and accuracy assessed using Certified Reference Material (CRM). Full details of the method and CRM results can be found in Milne et al. (2017).

2.3. Nutrients, phytoplankton, temperature and salinity

The dissolved macronutrients phosphate (PO_4^{3-}), silicic acid ($Si(OH)_4$ but referred to as Si hereafter) and nitrate (determined as nitrate + nitrite, NO_3^-) were determined in all samples for which trace metals were determined, in addition to samples collected from a stainless steel rosette. Macronutrients were determined using an AA III segmented-flow AutoAnalyzer (Bran & Luebbe) following colorimetric procedures (Woodward and Rees, 2001). Salinity, temperature and depth were measured using a CTD system (Seabird 911+) whilst dissolved O_2 was determined using a Seabird SBE 43 O_2 sensor. Salinity was calibrated on-board using discrete samples taken from the OTE bottles and an Autosal 8400B salinometer (Guildline) whilst dissolved O_2 was calibrated using a photometric automated Winkler titration system (Carritt and Carpenter, 1966). Mixed-layer depths (MLD) were calculated using the threshold method of de Boyer Montégut et al. (2014), where MLD is identified from a linear interpolation between near-surface density and the depth at which density changes by a threshold value (0.125 kg m^{-3}).

Measurements of phytoplankton pigment biomass and community structure were made on discrete samples collected using a 24 position stainless-steel CTD rosette equipped with 20 L OTE Niskin bottles. For chlorophyll-*a* analysis, samples were filtered (0.7 µm Whatman GF/F) and then the filters extracted overnight in 90 % acetone (Holm-Hansen et al., 1965). The chlorophyll-*a* extract was measured on a pre-calibrated (spinach chlorophyll-*a* standard, Sigma) Turner Designs Trilogy fluorometer. High performance liquid chromatography (HPLC) samples (0.5 – 2 L) for accessory pigment analyses were filtered (0.7 µm Whatman

GF/F), flash frozen in liquid nitrogen and stored at -80 °C prior to analysis using a Thermo HPLC system. The matrix factorization program CHEMTAX was used to estimate the contribution of taxonomic groups to total chlorophyll-*a* (Mackey et al., 1996). Concentrations of nanophytoplankton, *Synechococcus*, *Prochlorococcus* and photosynthetic picoeukaryotes were analysed by analytical flow cytometry (AFC) using a FACSort flow cytometer (Becton Dickenson, Oxford, UK) according to the methods described in Davey et al. (2008) and Zubkov et al. (2003).

3. Results and Discussion

3.1. Hydrographic setting and macronutrient distributions

The prominent waters masses along the D357 and JC068 transects (Fig. 2) were identified by their characteristic thermohaline and macronutrient properties (Sarmiento et al., 2004; Ansorge et al., 2005; Browning et al., 2014). Wyatt et al. (2014) provide a more detailed description of the JC068 hydrography along the entire GA10 section. Whilst we aim to compare the nearshore versus offshore distributions of micro- and macronutrients, note that sub-Antarctic mode water was not sampled for trace metals during the D357-2 late spring transect, and therefore only the early spring and summer values are discussed for SASW hereafter.

Surface mixed-layer

During all three transects the STF was identified by a sharp potential temperature (θ) gradient in the upper 200 m with the θ 15°C isotherm corresponding well to changes in macronutrient concentrations between STSW and SASW. North of the STF, mixed-layer macronutrient concentrations (Table 2) decreased in STSW between the three occupations of the transect. The largest relative depletion observed was for NO_3^- with a ~2.7-fold reduction in mean inventory concentration from 870 to 326 μmol m^{-3} between early spring and summer, whilst PO_4^{3-} and

Si concentrations were reduced 1.5- and 1.4-fold, respectively. The largest absolute depletion was observed for Si with a reduction of 848 µmol m^{-3} between early spring and summer. Conversely, summer SASW mixed-layer mean concentrations of NO_3^-, PO_4^{3-} and Si were relatively 1.6, 1.4 and 2.1-fold lower than early spring, respectively, whilst the largest absolute depletion of 1912 µmol m^{-3} was observed for NO_3^-. SASW mixed-layer concentrations of NO_3^- and PO_4^{3-} were at least 2.1-fold higher than for STSW during the study, whilst the Si concentration was at least 1.5-fold lower, highlighting the relative deficiencies in major nutrients between high and low latitude derived surface waters (Sarmiento et al., 2004; Moore, 2016).

Sub-surface waters

The Southern Ocean derived Sub-Antarctic Mode Water (SAMW) and underlying Antarctic Intermediate Water (AAIW) were identified using their characteristic core potential density ($\sigma\theta$ 26.8 kg m^{-3}) (Sarmiento et al., 2004; Palter et al., 2010) and thermohaline (S <34.4, θ >2.8ºC) properties (Fig. 2). Wyatt et al. (2014) have identified these water masses along this section between 200 and 500 m. During all three transects, low sub-surface (50 – 500 m) macronutrient concentrations were observed between 13 and 16°E, associated with a salinity maxima. The feature conforms to the mean locality and depth range of Agulhas water (Duncombe Rae, 1991), clearly highlighting the penetration of Indian Ocean water into northward flowing SAMW.

3.2. Zn and Co distributions of the Southeast Atlantic Ocean

Surface mixed-layer

Figure 3 shows the dZn and dCo distributions for the upper 500 m of the Southeast Atlantic for the D357 and JCO68 transects. For full-depth dZn distributions along JC068 refer to Wyatt et

al. (2014). In the surface mixed-layer, dZn and dCo concentrations ranged from 0.01 to 4.57 nM and 1 to 50 pM, respectively. The large range in dZn concentrations resulted from an apparent offshore transport of elevated dZn within STSW between 20 – 50 m during early spring (1.48 – 4.57 nM; Stns. 1 – 2) that was reduced by late spring (0.48 – 1.76 nM; Stns. 0.5 – 1.5) and was absent during summer (0.01 – 0.13 nM; Stns. 1 – 2). Similarly, but to a lesser extent, elevated dCo concentrations were observed in STSW between 10 and 50 m during early and late spring (15 – 50 pM), compared with summer (18 – 33 pM). Our findings are consistent with previous observations of elevated dissolved and particulate trace metals over the same depth range in waters close to South Africa, including Co, Fe, Mn, and Pb (Chever et al., 2010; Bown et al., 2011; Boye et al., 2012; Paul et al., 2015). We postulate that these trace metal enrichments can arise from either atmospheric inputs, and/or from the lateral advection of metal-enriched waters from the Agulhas Current (AC) and/or South African continental shelf, and discuss this further in Sect. 3.3. In SASW, mixed-layer dZn and dCo concentrations ranged from 0.01 to 0.25 nM and 3 to 18 pM, respectively, during the study, significantly lower than STSW values, with the lowest concentrations observed during the summer transect (Table 2).

Sub-surface waters

During the early spring D357-1 transect, elevated dZn and dCo concentrations were observed between the surface mixed-layer and 500 m (1.48–3.85 nM and 39–62 pM, respectively) at the station closest the South African continent (Stn. 1). Here, the highest dZn concentrations were associated with the dZn-enriched waters (20–55 m) described above for the surface mixed-layer. During the late spring D357-2 transect, the near-shore (Stns. 0.5–1) dZn concentrations were lower (0.31–1.76 nM) whilst dCo remained similar to early spring values (27–57 pM). During summer, near-shore (Stn. 1) sub-surface dZn concentrations were markedly lower (0.03–0.50 nM) than spring values whilst dCo concentrations (17–52 pM) were only

marginally lower. In offshore waters, sub-surface dZn concentrations ranged from 0.01 to 1.01 nM across all three transects with extremely low values in the upper 400 m (0.22 ± 0.21 nM) and the highest values between 400 and 500 m. The absence of a significant return path for dZn with SAMW to waters above 400 m at this latitude (Wyatt et al., 2014; Vance et al., 2017) is likely an important control on dZn distributions across all three transects. In contrast, dCo concentrations were depleted in the upper 200 m (1–35 pM) and elevated in SAMW (23–56 pM) suggesting that these Southern Ocean derived waters also play an important role in upper water column dCo distributions of the South Atlantic.

To assess whether seasonal changes in subsurface supply could influence dissolved Zn and Co concentrations in the upper water column of the Southeast Atlantic, we examined the metal versus PO_4^{3-} distributions of underlying SAMW and AAIW. Throughout this paper metal:PO_4^{3-} will be used to indicate an uptake remineralisation ratio derived from a regression slope, whilst metal/PO_4^{3-} will denote a concentration ratio. Figure 4 and supplementary table 1 show how the dZn:PO_4^{3-} regression slope for SAMW and AAIW varied little between the three transects. These slopes are a function of the pre-formed micro- and macronutrient concentrations and the uptake/remineralisation ratio of the sources waters, as well as mixing during advection between the Southern Ocean and South Atlantic (Vance et al., 2017; Middag et al., 2018). The dZn:PO_4^{3-} slopes steepen with the introduction of AAIW with higher dZn/PO_4^{3-} concentration ratios, yet it is the relatively shallow slopes of overlying SAMW that imply a low, and relatively consistent, subsurface supply of dZn to STSW and SASW of the South Atlantic (Wyatt et al., 2014). The shallower waters overlying SAMW clearly show elevated dZn concentration, specifically during the spring transects, compared with what could be delivered if subsurface supply was the dominant source governing dZn availability in surface waters (Fig. 4). It is therefore unlikely that a change in subsurface supply from underlying SAMW is responsible for the change in dZn inventories of STSW and SASW between the three transects.

Similarly, the dCo:PO_4^{3-} regression slope varied little between the three transects (Fig. 4 and Supp. Table 1). In dCo:PO_4^{3-} space, a single slope can be fit to SAMW and AAIW with no net scavenging effect on dCo distribution over the upper 1000 m. Like dZn, the waters overlying SAMW displayed spring dCo concentrations elevated above that potentially delivered via SAMW supply. During summer however, SAMW may provide a subsurface source of dCo (Fig. 4c) to overlying waters highlighting how Southern Ocean derived waters may play important, yet different, roles in upper water column metal distributions of the Southeast Atlantic.

3.3. Shelf derived sources of Zn and Co

Potential sources of trace metals to surface waters of the Southeast Atlantic include atmospheric inputs from South Africa and Patagonia (Chance et al., 2015; Menzel Barraqueta et al., 2019) as well as interactions with shelf and slope waters of the Agulhas Bank (Bown et al., 2011; Boye et al., 2012; Paul et al., 2015). During the D357 spring transects, elevated mixed-layer dZn and dCo concentrations (up to 4.57 nM and 50 pM, respectively; Sect. 3.2) were observed at stations closest the Agulhas Bank shelf and slope (Stns. 0.5, 1, 1.5 and 2). Here, we compare these metal elevations with respect to the aforementioned sources. Firstly, we encountered only brief, light rain during the study, thus minimal wet deposition of atmospheric aerosol. By combining the median atmospheric dry deposition flux for soluble Zn and Co for the Southeast Atlantic (Zn 6.0 and Co 0.05 nmol m^{-2} d^{-1}; Chance et al., 2015) with the mean mixed-layer depth (34 m) for STSW during D357, dust dissolution is estimated to add approximately 5.5 and 0.05 nmol m^{-3} dZn and dCo, respectively, over a one month period. These inputs are low compared with the mixed-layer metal inventories, representing <1 % of dZn and dCo concentration in STSW during the D357 transects (Table 2), and would not be sufficient to generate distinct mixed-layer maxima. It is likely, therefore, that the dZn and dCo

elevations originated from the advection of metal-enriched waters from the western Agulhas Bank, a region identified as a distinct source of both dissolved and particulate trace metals to the Southeast Atlantic (Chever et al., 2010; Bown et al., 2011; Boye et al., 2012; Paul et al., 2015), and/or from the leakage of Indian Ocean water into the Southeast Atlantic via the AC. The detachment of Agulhas rings and filaments from the AC during its retroflection back towards the Indian Ocean constitutes a source of Pb to the surface Southeast Atlantic along the D357 transects (Paul et al., 2015). Whilst we observed elevated mixed-layer dZn and dCo at ~15ºE during both D357 transects, the absence of metal enrichment across the depth of the AC salinity maxima (Figs. 2 and 3) suggests that the signal must be entrained from elsewhere. Furthermore, dZn concentrations from the AC along the east coast of South Africa do not exceed 0.5 nM in the upper 200 m (Gosnell et al., 2012). It is therefore likely that the dZn and dCo enrichment was derived from the Agulhas Bank. The AC has been shown to meander over, and interact with, the Agulhas Bank, forming eddies and filaments on the shoreward edge of the AC proper, that tend to move northwards along the western shelf edge and into the Southeast Atlantic (Lutjeharms and Cooper, 1996; Lutjeharms, 2007), potentially delivering shelf-derived sedimentary material. We found no evidence of a fluvial signature in our data, and no significant fluvial source for trace elements to our study region has been reported in the literature. We focus here on the more likely scenario of sedimentary inputs as the driver of mixed-layer dZn and dCo elevations at the shelf and slope stations during D357. Despite no available particulate trace metal data for the D357-1 early spring transect for direct comparison with the highest dZn and dCo elevations, we observed elevated mixed-layer particulate Zn (pZn; 0.08–1.40 nM) and Co (pCo; 8–49 pM) at stations closest South Africa during the D357-2 late spring transect (Stns. 0.5, 1 and 1.5, Fig. S1), coincident with elevated dZn (0.05–1.82 nM) and dCo (1–43 pM). Furthermore, for the upper 500 m at stations 0.5 and 1, we found strong positive correlations between particulate aluminium and titanium (pAl:pTi, slope 41.7

mol mol^{-1}, Pearson's *r* 0.99, *n* = 15), as well as particulate Fe and titanium (pFe:pTi, slope 10.2 mol mol^{-1}, Pearson's *r* 0.99, *n* = 15), indicative of a strong lithogenic source. Whilst there are presently no South African sedimentary data against which we can compare our water column values, our pAl:pTi and pFe:pTi slope ratios are in excess of upper crustal mole ratios (34.1 and 7.3 mol mol^{-1}, respectively; Mclennan, 2001). These 500 m ratios are also steeper than the aggregate slopes for the full depth Atlantic Ocean away from hydrothermal sources (32.1 and 7.4 mol mol^{-1}, Pearson's *r* >0.97, *n* = 593, Schlitzer, 2018). Given the refractory nature of lithogenic pTi across diverse oceanic environments (Ohnemus and Lam, 2015), this may suggest the resuspension and dissolution of Agulhas Bank sediments enriched in dAl and dFe, followed by westward offshore transport, a common feature of the Bank's physical circulation during spring and summer (Largier et al., 1992). Such processes may in turn provide an additional source of dZn and dCo to STSW of the Southeast Atlantic. For example, Little et al. (2016) proposed that oxygen-deficient, organic-rich, continental margin sediments may constitute a significant global sink within the marine Zn cycle. These sediments could additionally provide a local source of dZn following remineralisation. Recent model outputs have likewise highlighted oxygen-deficient, boundary sediments as a dominant external source of Co to the oceans (Tagliabue et al., 2018). Given that oxygen depleted (<45 µM) bottom waters are prevalent across the western Agulhas Bank (Chapman and Shannon, 1987; Chapman, 1988), considered to arise from high organic matter input to sediments and its bacterial decomposition, a sedimentary source of dZn and dCo appears likely.

3.4. Trace metal stoichiometry of the upper Southeast Atlantic

In addition to seasonal variations in the lateral advection of continentally derived trace metals, the lower dZn and dCo concentrations in STSW during summer, compared with spring, likely reflect differences in biological utilisation. Here, we examine the micro- and macronutrient

concentration inventories to assess the trace metal stoichiometry of the Southeast Atlantic over seasonal timescales. The data were grouped into STSW and SASW regimes, with STSW defined by $\theta \geq 15°C$. This isotherm was located at a mean depth of 144 ± 96 m across the study, compared with a mean mixed-layer depth of 39 ± 10 m, and thus the inventories for SASW were determined over this depth for comparison with STSW (Table 2). Early and late spring STSW samples in the depth range 20 - 55 m that clearly exhibited continentally derived elevated dZn and dCo were removed from the analysis in order to compare stoichiometry with respect to biological processes. For SASW, micronutrient sampling did not occur during late spring and therefore only early spring and summer values are compared.

Distinct temporal trends in the stoichiometric relationship with PO_4^{3-} were evident for both dZn and dCo (Fig. 4). Within STSW, the dZn/PO_4^{3-} inventory ratio ranged from 699 to 1876 µmol mol^{-1} (Table 2) with the highest value observed during early spring and the lowest during summer. Combined with summer dZn concentrations 4-fold lower than early spring, this suggests strong biological uptake of dZn alongside PO_4^{3-} between seasons. In contrast, lower dZn/PO_4^{3-} ratios of 372 and 188 µmol mol^{-1} were observed in SASW during early spring and summer, respectively. Here, the absolute change in dZn concentration between spring and summer was lower than for STSW, but was greater for PO_4^{3-}, likely reflecting the increased availability of PO_4^{3-} in these Southern Ocean derived waters (Table 2) and an open-ocean phytoplankton community that have lower trace metal requirements than their counterparts north of the STF. Such dZn/PO_4^{3-} ratios sit at the lower end of cellular Zn/P reported for the diatom and haptophyte-type phytoplankton typical of this region (~100 – 1100 µmol mol^{-1}; Twining and Baines, 2013 and refs. therein), highlighting the importance of micronutrient processes with respect to Zn availability.

In contrast to dZn, the spatiotemporal variation observed for STSW dCo/PO_4^3 was small with ratios ranging from 82 to 129 µmol mol^{-1} (Table 2), likely reflecting external inputs to the

oceans and biological Co requirements that are typically 4-fold less than for Zn (Ho et al., 2003; Roshan et al., 2016; Hawco et al., 2018). The STSW dCo/PO_4^{3-} ratio decreased between early and late spring transects, potentially in part due to the westward expansion of STSW during late spring (Fig. 2) and subsequent mixing with SASW depleted in dCo relative to PO_4^{3-} (Fig. 3). This dilution is likely also true of dZn and Si, yet their STSW concentration inventories may be sufficiently high as to mask this effect. Unfortunately, an insufficient quantity of late spring SASW data are available with which to affirm this postulation. The highest dCo/PO_4^{3-} ratio was observed during summer due to the preferential biological removal of PO_4^{3-} relative to dCo.

In SASW, dCo/PO_4^{3-} was consistently low with ratios of 23 and 26 μmol mol^{-1} for early spring and summer, respectively. Much higher inventory ratios of ~580 μmol mol^{-1} can be calculated over similar depths for open-ocean North Atlantic waters (GA03 Stns. 11-20, Schlitzer et al., 2018), likely reflecting an elevated atmospheric Co input and/or an extremely low surface PO_4^{3-} inventory (Wu et al., 2000; Martiny et al., 2019).

Our results provide evidence for the greater availability and preferential removal of dZn relative to dCo in the upper water column the Southeast Atlantic based on STSW dZn/dCo inventory ratios of 19, 17 and 5 mol mol^{-1} for the three transects and SASW ratios of 13 and 7 mol mol^{-1} for early spring and summer, respectively (Table 2). With relatively consistent inter-seasonal dCo inventories for STSW and SASW, indicating a more balanced ecophysiological regime with regard to dCo organisation, the change in dZn/dCo inventory stoichiometries principally reflects changes in dZn concentration. We postulate that the inter-seasonal variations in dZn and dCo availability and stoichiometry of the Southeast Atlantic reflect changes in the relative nutritional requirement of resident phytoplankton and/or biochemical substitution of Zn and Co to meet nutritional demand.

3.5. Phytoplankton controls on trace metal ecological stoichiometry

Here we discuss the principle phenomena that together likely explain our observations of seasonally decreasing dZn/dCo inventory stoichiometries in STSW and SASW of the Southeast Atlantic: i.e. the preferential removal of dZn, relative to dCo, leading to low dZn availability, and differences in phytoplankton assemblages with different cellular metal requirements.

Satellite images show elevated surface chlorophyll concentrations across the Southeast Atlantic STF, compared with waters further north and south, with peak concentrations observed during summer in January 2012 (Fig. 1). Profiles of total chlorophyll-*a* concentration (Fig. S2) also show maximum summer values in the upper water column of STSW (1.02 mg m^{-3}) and SASW (0.49 mg m^{-3}) compared with spring values (<0.61 and <0.36 mg m^{-3}, respectively). This is consistent with the hypothesis that increasing irradiance, coupled with shallower mixed-layer depths (de Boyer Montégut et al., 2004), result in enhanced growth conditions across the STF between September and February (Browning et al., 2014). Diagnostic pigment analyses (Fig. 5a) indicated that eukaryotic nanophytoplankton, specifically *Phaeocystis*-type haptophytes, dominated the early spring STSW chlorophyll-*a* content (73 %) but with a reduced contribution during summer (20 %). Maximum growth rates for cultured *Phaeocystis antarctica* have been achieved under elevated Zn concentrations (Saito and Goepfert, 2008), and thus, the dominance of this haptophyte would likely contribute to the removal of dZn between spring and summer. Furthermore, an increased summer diatom contribution (13 % chlorophyll-*a* compared with near zero during spring transects) would have further reduced the dZn inventory, with diatoms having at least 4-fold higher cellular Zn/P ratios than co-occurring cell types (Twining and Baines, 2013).

The fact that both *Phaeocystis* and diatomaceous nanophytoplankton maintain a contribution to the summer STSW chlorophyll-*a* complement, when dZn availability is low, is intriguing.

Both *P. antarctica* and the large, coastal diatoms *Thalassiosira pseudonana* and *Thalassiosira weissflogii* have been shown to be growth limited in culture by free Zn^{2+} concentrations ≤10 pM (Sunda and Huntsman, 1992; Saito and Goepfert, 2008). A simple estimate of summer STSW free Zn^{2+} availability, based on North Atlantic organic complexation data (>96 %; Ellwood and Van den Berg, 2000), indicated free Zn^{2+} averaged $6.3 \pm 5.3u_c$ pM, suggesting the potential for growth limitation of these phytoplankton. In addition, when comparing the Southeast Atlantic dZn stoichiometry with the cellular requirements of phytoplankton grown under growth rate limiting conditions (Fig. 6), we found summer STSW dZn/PO_4^{3-} to be in deficit of the requirements of coastal *T. pseudonana* but not those of the smaller, open-ocean diatom *T. oceanica*. The variation in cellular Zn/P between small and large phytoplankton is related to the higher surface-area-to-volume ratio of smaller cells, and the limitation of diffusive uptake rates at low Zn^{2+} concentrations (Sunda and Huntsman, 1995). This would suggest that the lower dZn availability in summer STSW should influence phytoplankton species composition by selecting for smaller organisms with lower cellular Zn requirements, and confirmed by a ratio of picophytoplankton to nanophytoplankton at least 4-fold higher during summer compared with spring values. The comparison further implies that the presence of *Phaeocystis* and diatoms in summer STSW may be linked with their metabolic Zn-Co-Cd substitution capability, potentially allowing them to overcome some portion of their Zn deficiency. Largely connected to carbonic anhydrase enzymes, several species of eukaryotic phytoplankton are capable of biochemical substitution of Zn, Co or Cd to maintain optimal growth rates under low trace metal conditions (Price and Morel, 1990; Sunda and Huntsman, 1995; Lee and Morel, 1995; Lane and Morel, 2000; Xu et al., 2007; Saito and Goepfert, 2008; Kellogg et al., 2020). For example, metabolic substitution of Co in place of Zn has been observed to support the growth of *P. antarctica*, *T. pseudonana* and *T. weissflogii* in media with Zn^{2+} <3 pM (Sunda and Huntsman, 1995; Saito and Goepfert, 2008; Kellogg et al., 2020).

Thus, the lower mixed-layer dCo inventory of summer STSW, relative to early spring, may be in part related to enhanced dCo uptake through biochemical substitution alongside the growth of phytoplankton with distinct Co requirements.

In contrast to *Phaeocystis*, *E. huxleyi*-type haptophytes were near-absent in spring STSW (<5 % chlorophyll-*a*; Fig. 5a) and increased in contribution during summer (18 %). *Emiliania huxleyi* appear to have a biochemical preference for Co over Zn (Xu et al., 2007), which could potentially be a contributing factor to the increased fraction of this haptophyte in summer STSW. Based on Co organic complexation data for Southeast Atlantic STSW (>99 %; Bown et al., 2012), however, even the maximum dCo concentration of 56 pM (estimated free Co^{2+} 0.56 ± 0.11u_c pM) observed for STSW during this entire study would limit the growth of cultured *E. huxleyi* in the absence of Zn or Cd (Sunda and Huntsman, 1995; Xu et al., 2007). This is supported by inter-seasonal dCo/PO_4^{3-} stoichiometries in deficit of the cellular requirements of cultured *E. huxleyi* (Fig. 6). Despite this, Xu et al. (2007) showed that *E. huxleyi* can maintain significant growth at only 0.3 pM Co^{2+} in the presence of Zn, with the limitation by, and substitution of these metals reported to occur over a range of free ion concentrations (0.2–5 pM) that is relevant to summer conditions of the Southeast Atlantic. This assessment implies an additional need for Zn in phytoplankton nutrition due to low dCo availability throughout the Southeast Atlantic, which may accelerate the decrease in dZn/dCo inventory ratio between seasons.

The elevated summer STSW chlorophyll-*a* concentrations were accompanied by increased cell concentrations of the *Synechococcus* and *Prochlorococcus* (up to 100 and 400 cells μL^{-1}, respectively) relative to early spring abundance (Fig. 5b). This pattern suggests an inter-seasonal community shift towards smaller picocyanobacterial cells that is coincident with decreased dZn availability. *Synechococcus* and *Prochlorococcus* are thought to have little or no Zn requirement and relatively low Co requirements (growth limited by ≤0.2 pM Co^{2+}; Sunda

and Huntsman, 1995; Saito et al., 2002). This, alongside their small cell size, hence greater capacity for acquiring fixed nitrogen under conditions where this nutrient is depleted, may allow these prokaryotes to flourish following depletion and export of Zn associated with *Phaeocystis* and diatom blooms. This supposition is supported by a persistently high abundance of *Synechococcus* and *Prochlorococcus* (>1000 cells μL^{-1}), relative to eukaryotic nanophytoplankton, in the dZn depleted surface waters of the Costa Rica Dome (Saito et al., 2005; Ahlgren et al., 2014; Chappell et al., 2016). Here, surface dCo concentrations were maintained above that of surrounding waters by the biological production of Co-binding ligands (Saito et al., 2005). The increased abundance of these prokaryotic autotrophs in summer STSW of the Southeast Atlantic may have also contributed to the inter-seasonal decrease in dCo inventory.

In contrast to STSW, cells counts of eukaryotic phytoplankton and prokaryotic cyanobacteria in SASW varied little between early spring and summer (Fig. 5b), indicative of a more balanced ecophysiological regime. The fractional contribution of *Phaeocystis* (Fig. 5a), the dominant contributor to the SASW chlorophyll-*a* complement, was similar between transects at 54 and 44 %, respectively, whilst the contribution of *E. huxleyi* increased from 19 to 33 % between spring and summer, respectively. Whilst it is proposed that the low Fe supply rate to these waters provides a dominant control on phytoplankton biomass and composition (Browning et al., 2014), low dZn and dCo availability may also be important drivers of such change. The Summer SASW dZn inventory ($0.08 \pm 0.07u_c$ nM) and stoichiometry with PO_4^{3-} (Fig. 6) indicate growth limiting conditions for *Phaeocystis* and *E. huxleyi* in the absence of cambialistic metabolism (Sunda and Huntsman., 1995; Saito and Goepfert, 2008; Xu et al., 2007). The presence of these phytoplankton therefore indicates Zn biochemical substitution occur in oceanic waters of the Southeast Atlantic. A lower Co half-saturation growth constant for cultured *P. antarctica* (K_m = ~0.2 pM Co^{2+}), compared with *E. huxleyi* (K_m = ~3.6 pM

Co^{2+}), further suggests that *Phaeocystis* species may more effectively occupy low dZn and dCo environments (Saito and Goepfert, 2008), such as SASW of the South Atlantic.

Conversely, the absence of a significant diatom contribution to summer SASW chlorophyll-*a* (Fig. 5a), relative to early spring, is surprising as the summer dZn/PO_4^{3-} inventory ratio is in excess of the cellular Zn/P requirements of typical oceanic diatoms such as *T. oceanica* (Fig. 6). Furthermore, whilst the dCo/PO_4^{3-} ratio of summer SASW is in deficit of the cellular Co/P below which growth limitation of *T. oceanica* may occur, this species has been shown to grow effectively at Co^{2+} <0.1 pM in culture in the presence of Zn (Sunda and Huntsman, 1995). The low diatom fractional contribution to summer SASW may be instead related to low Fe availability (Browning et al., 2014) and stress-induced Si exhaustion. In support of this, we calculate summer SASW mixed-layer Si concentrations (0.9 ± 0.3 µM) to be 50 % of early spring values (1.8 ± 0.2 µM) with a dissolved NO_3^-/Si stoichiometry of 3.8 mol mol^{-1} close to the 4 mol mol^{-1} shown to limit diatom growth in culture (Gilpin et al., 2004), and in contrast to the 2.9 mol mol^{-1} calculated for early spring.

3.6. Conclusion

We report the distributions of dZn and dCo in the upper water column of sub-tropical and sub-Antarctic waters of the Southeast Atlantic during austral spring and summer periods. We identify an apparent continental source of dZn and dCo to sub-tropical waters at depths between 20 – 55 m, derived from sedimentary inputs from the Agulhas Bank. In contrast, open-ocean sub-Antarctic surface waters displayed largely consistent inter-seasonal mixed-layer dZn and dCo concentrations indicating a more balanced ecophysiological regime with regard to their organisation. The vertical distributions of dZn and dCo in the upper water column were similar to that of PO_4^{3-} indicating biological drawdown in surface waters and mixing with underlying Southern ocean-derived waters travelling equatorward significantly influences their

distribution. Absolute trace metal concentrations alongside concentration inventory ratios suggest the preferential utilization of dZn, relative to dCo, in the Southeast Atlantic with dZn/dCo decreasing from 19 to 5 mol mol^{-1} between early spring and summer in STSW and from 13 to 7 mol mol^{-1} in SASW. This pattern is consistent with our understanding of the cellular requirement of phytoplankton (Twining and Baines, 2013). The inter-seasonal removal of dZn results in summer concentrations that are potentially growth limiting for certain phytoplankton species estimated to be present in these waters by diagnostic pigment analyses. We therefore suggest cambialistic metabolic substitution between Zn and Co, and potentially Cd, is an important factor regulating the growth, distribution and diversity of phytoplankton in the Southeast Atlantic.

Data availability. The trace metal and macronutrient data sets used for analyses in this study are available at https://www.bodc.ac.uk/geotraces/data/idp2017/ (GEOTRACES GA10) and phytoplankton data at https://www.bodc.ac.uk/.

Competing interests. The authors declare that they have no conflict of interest.

Author contribution. MCL and EPA acquired the funding. NJW, MCL, AM, TJB, EMSW, and HAB collected samples at sea. NJW conducted the Zn and Co measurements, EMSW the macronutrient measurements and TJB the phytoplankton measurements. NJW prepared the manuscript with significant contributions from all co-authors.

Acknowledgments. We thank the officers, crew, technicians and scientists of the *RRS James Cook* for their help on the UK-GEOTRACES D357 and JC068 cruises. This work was funded

by the UK-GEOTRACES National Environmental Research Council (NERC) Consortium Grant (NE/H006095/1 (MCL & HAB) & NE/H004475/1 (EPA)).

References

Ahlgren, N. A., Noble, A. E., Patton, A. P., Roache-Johnson, K., Jackson, L., Robinson, D., McKay, C., Moore, L. R., Saito, M. A., and Rocap, G.: The unique trace metal and mixed layer conditions of the Costa Rica upwelling dome support a distinct and dense community of Synechococcus, Limnol. Oceanogr., 59, 2166-2184, doi:10.4319/lo.2014.59.6.2166, 2014.

Ansorge, I. J., Speich, S., Lutjeharms, J. R. E., Goni, G. J., Rautenbach, C. J. D., Froneman, P. W., Rouault, M., and Garzoli, S.: Monitoring the oceanic flow between Africa and Antarctica: Report of the first Goodhope cruise, S. Afr. J. Sci., 101, 29-35, 2005.

Bertrand, E. M., Saito, M. A., Rose, J. M., Riesselman, C. R., Lohan, M. C., Noble, A. E., Lee, P. A., and DiTullio, G. R.: Vitamin b12 and iron colimitation of phytoplankton growth in the Ross Sea, Limnol. Oceanogr., 52, 1079-1093, doi:10.4319/lo.2007.52.3.1079, 2007.

Bown, J., Boye, M., Baker, A., Duvieilbourg, E., Lacan, F., Le Moigne, F., Planchon, F., Speich, S., and Nelson, D. M.: The biogeochemical cycle of dissolved cobalt in the Atlantic and the Southern Ocean south off the coast of South Africa, Mar. Chem., 126, 193-206, doi:10.1016/j.marchem.2011.03.008, 2011.

Bown, J., Boye, M., and Nelson, D. M.: New insights on the role of organic speciation in the biogeochemical cycle of dissolved cobalt in the southeastern Atlantic and the Southern Ocean, Biogeosciences, 9, 2719–2736, doi:10.5194/bg-9-2719-2012, 2012.

Boye, M., Wake, B. D., Garcia, P. L., Bown, J., Baker, A. R., and Achterberg, E. P.: Distributions of dissolved trace metals (Cd, Cu, Mn, Pb, Ag) in the southeastern Atlantic and the Southern Ocean, Biogeosciences, 9, 3231-3246, doi:10.5194/bg-9-3231-2012, 2012.

Browning, T. J., Bouman, H. A., Moore, C. M., Schlosser, C., Tarran, G. A., Woodward, E. M. S., and Henderson, G. M.: Nutrient regimes control phytoplankton ecophysiology in the South Atlantic, Biogeosciences, 11, 463-479, doi:10.5194/bg-11-463-2014, 2014.

Browning, T. J., Achterberg, E. P., Rapp, I., Engel, A., Bertrand, E. M., Tagliabue, A., and Moore, C. M.: Nutrient co-limitation at the boundary of an oceanic gyre, Nature, 551, 242-246, doi:10.1038/nature24063, 2017.

Cannizzaro, V., Bowie, A.R., Sax, A., Achterberg, E. P., Worsfold, P. J.: Determination of cobalt and iron in estuarine and coastal waters using flow injection with chemiluminescence detection, Analyst, 125, 51-57, doi:10.1039/A907651d, 2000.

Carritt, D. E., and Carpenter, J. H.: Comparison and evaluation of currently employed modifications of the Winkler method for determining dissolved oxygen in seawater; a nasco report, J. Mar. Res., 24, 286 - 319, 1966.

586 Chance, R., Jickells, T. D., and Baker, A. R.: Atmospheric trace metal concentrations,
587 solubility and deposition fluxes in remote marine air over the south-east Atlantic, Mar. Chem.,
588 177, 45-56, doi:10.1016/j.marchem.2015.06.028, 2015.

589 Chapman, P.: On the occurrence of oxygen-depleted water south of Africa and its implications
590 for Agulhas-Atlantic mixing, S. Afr. J. Marine Sci., 7, 267-294,
591 doi:10.2989/025776188784379044, 1988.

592 Chapman, P., and Shannon, L. V.: Seasonality in the oxygen minimum layers at the extremities
593 of the Benguela system, S. Afr. J. Marine Sci., 5, 85-94, doi:10.2989/025776187784522162,
594 1987.

595 Chappell, P. D., Vedmati, J., Selph, K. E., Cyr, H. A., Jenkins, B. D., Landry, M. R., and
596 Moffett, J. W.: Preferential depletion of zinc within Costa Rica upwelling dome creates
597 conditions for zinc co-limitation of primary production, J. Plankton Res., 38, 244-255,
598 doi:10.1093/plankt/fbw018, 2016.

599 Chever, F., Bucciarelli, E., Sarthou, G., Speich, S., Arhan, M., Penven, P., and Tagliabue, A.:
600 Physical speciation of iron in the Atlantic sector of the Southern Ocean along a transect from
601 the subtropical domain to the Weddell Sea Gyre, J. Geophys. Res-Oceans, 115, C10059,
602 doi:10.1029/2009jc005880, 2010.

603 Cox, A., and Saito, M.: Proteomic responses of oceanic Synechococcus WH8102 to phosphate
604 and zinc scarcity and cadmium additions, Front Microbiol, 4, doi:10.3389/fmicb.2013.00387,
605 2013.

606 Cullen, J. T., and Sherrell, R. M.: Effects of dissolved carbon dioxide, zinc, and manganese on
607 the cadmium to phosphorus ratio in natural phytoplankton assemblages, Limnol. Oceanogr.,
608 50, 1193-1204, doi:10.4319/lo.2005.50.4.1193, 2005.

609 Cutter, G., Anderssen, P., Codispoti, L., Croot, P. L., Francois, R., Lohan, M. C., Obata, H.,
610 and Rutgers van der Leoff, M.: Sampling and sample-handling protocols for GEOTRACES
611 cruises, geotraces.org. 2010.

612 Davey, M., Tarran, G. A., Mills, M. M., Ridame, C., Geider, R. J., and LaRoche, J.: Nutrient
613 limitation of picophytoplankton photosynthesis and growth in the tropical North Atlantic,
614 Limnol. Oceanogr., 53, 1722–1733, doi:10.4319/lo.2008.53.5.1722, 2008

615 de Boyer Montégut, C., Madec, G., Fischer, A. S., Lazar, A., and Iudicone, D.: Mixed layer
616 depth over the global ocean: An examination of profile data and a profile-based climatology,
617 J. Geophys. Res-Oceans, 109, C12003, doi:10.1029/2004jc002378, 2004.

618 Dulaquais, G., Boye, M., Middag, R., Owens, S., Puigcorbe, V., Buesseler, K., Masqué, P.,
619 Baar, H. J., and Carton, X.: Contrasting biogeochemical cycles of cobalt in the surface western
620 Atlantic Ocean, Global Biogeochem. Cy., 28, 1387–1412, doi:10.1002/2014GB004903, 2014.

621 Duncombe Rae, C. M.: Agulhas retroflection rings in the South Atlantic Ocean: An overview,
622 S. Afr. J. Marine Sci., 11, 327-344, doi:10.2989/025776191784287574, 1991.

623 Ellwood, M. J., and Van den Berg, C. M. G.: Zinc speciation in the Northeastern Atlantic
624 Ocean, Mar. Chem., 68, 295-306, doi:10.1016/S0304-4203(99)00085-7, 2000.

Franck, V. M., Bruland, K. W., Hutchins, D. A., and Brzezinski, M. A.: Iron and zinc effects on silicic acid and nitrate uptake kinetics in three high-nutrient, low-chlorophyll (HNLC) regions, Mar. Ecol. Prog. Ser., 252, 15-33, doi:10.3354/meps252015, 2003.

Gilpin, L. C., Davidson, K., and Roberts, E.: The influence of changes in nitrogen: silicon ratios on diatom growth dynamics, J. Sea Res., 51, 21-35, doi:10.1016/j.seares.2003.05.005, 2004.

Gosnell, K. J., Landing, W. M., and Milne, A.: Fluorometric detection of total dissolved zinc in the southern Indian Ocean, Mar. Chem., 132, 68-76, doi:10.1016/j.marchem.2012.01.004, 2012.

Hawco, N. J., and Saito, M. A.: Competitive inhibition of cobalt uptake by zinc and manganese in a Pacific Prochlorococcus strain: Insights into metal homeostasis in a streamlined oligotrophic cyanobacterium, Limnol. Oceanogr., 63, 2229-2249, doi:10.1002/lno.10935, 2018.

Hawco, N.J., Lam, P.J., Lee, J.M., Ohnemus, D.C., Noble, A.E., Wyatt, N.J., Lohan, M.C., and Saito M.A.: Cobalt scavenging in the mesopelagic ocean and its influence on global mass balance: synthesizing water column and sedimentary fluxes, Mar. Chem., 201, 151-166, doi.org/10.1016/j.marchem.2017.09.001, 2018.

Ho, T. Y., Quigg, A., Finkel, Z. V., Milligan, A. J., and Wyman, K.: The elemental composition of some marine phytoplankton, J. Phycol., 39, 1145-59, doi.org/10.1111/j.0022-3646.2003.03-090.x.

Holm-Hansen, O., Lorenzen, C. J., and Holmes, J. D. H.: Fluorometric determination of chlorophyll, ICES J. Mar. Sci., 30, 3-15, doi.org/10.1093/icesjms/30.1.3, 1965.

Ito, T., Parekh, P., Dutkiewicz, S., and Follows, M. J.: The Antarctic circumpolar productivity belt, Geophys. Res. Lett., 32, L13604, doi:10.1029/2005gl023021, 2005.

Jakuba, R. W., Moffett, J. W., and Dyhrman, S. T.: Evidence for the linked biogeochemical cycling of zinc, cobalt, and phosphorus in the western north Atlantic Ocean, Global Biogeochem. Cy., 22, GB4012, doi:10.1029/2007GB003119, 2008.

Jakuba, R. W., Saito, M. A., Moffett, J. W., and Xu, Y.: Dissolved zinc in the subarctic North Pacific and Bering Sea: Its distribution, speciation, and importance to primary producers, Global Biogeochem. Cy., 26, GB2015, doi:10.1029/2010gb004004, 2012.

Kellogg, M.M., Mcllvin, M.R., Vedamati, J.,Twining, B.S., Moffett, J.W., Marchetti, A., Moran, D.M., and Saito, M.A.: Efficient zinc/cobalt inter-replacement in northeast Pacific diatoms and relationship to high surface dissolved Co:Zn ratios, Limnol. Oceanogr., 9999, 1-26, doi:10.1002/lno.11471, 2020.

Lane, T. W., and Morel, F. M. M.: Regulation of carbonic anhydrase expression by zinc, cobalt, and carbon dioxide in the marine diatom Thalassiosira weissflogii, Plant Physiol., 123, 345-352, doi:10.1104/Pp.123.1.345, 2000.

Largier, J. L., Chapman, P., Peterson, W. T., and Swart, V. P.: The western Agulhas Bank: circulation, stratification and ecology, S Afr J Marine Sci, 12, 319-339, doi:10.2989/02577619209504709, 1992.

Leblanc, K., Hare, C. E., Boyd, P. W., Bruland, K. W., Sohst, B., Pickmere, S., Lohan, M. C., Buck, K., Ellwood, M., and Hutchins, D. A.: Fe and Zn effects on the Si cycle and diatom community structure in two contrasting high and low-silicate HNLC areas, Deep-Sea Res. Pt I, 52, 1842-1864, doi:10.1016/j.dsr.2005.06.005, 2005.

Lee, J. G., and Morel, F. M. M.: Replacement of zinc by cadmium in marine phytoplankton, Mar. Ecol. Prog. Ser., 127, 305-309, doi:10.3354/Meps127305, 1995.

Little, S. H., Vance, D., McManus, J., and Severmann, S.: Key role of continental margin sediments in the oceanic mass balance of Zn and Zn isotopes, Geology, 44, 207-210, doi:10.1130/G37493.1, 2016.

Lutjeharms, J. R. E.: Three decades of research on the greater Agulhas Current, Ocean Sci., 3, 129-147, doi:10.5194/os-3-129-2007, 2007.

Lutjeharms, J. R. E., and Cooper, J.: Interbasin leakage through Agulhas current filaments, Deep-Sea Res. Pt I, 43, 213-238, doi:10.1016/0967-0637(96)00002-7, 1996.

Mackey, M. D., Mackey, D. J., Higgins, H. W., and Wright, S. W.: Chemtax - a program for estimating class abundances from chemical markers: Application to HPLC measurements of phytoplankton, Mar. Ecol. Prog. Ser., 144, 265-283, doi:10.3354/meps144265, 1996.

Mahaffey, C., Reynolds, S., Davis, C. E., and Lohan, M. C.: Alkaline phosphatase activity in the subtropical ocean: Insights from nutrient, dust and trace metal addition experiments, Front. Mar. Sci., 1, doi:10.3389/fmars.2014.00073, 2014.

Martiny, A. C., Lomas, M. W., Fu, W., Boyd, P. W., Chen, Y. L., Cutter, G. A., Ellwood, M. J., Furuya, K., Hashihama, F., Kanda, J., Karl, D. M., Kodama, T., Li, Q. P., Ma, J., Moutin, T., Woodward, E. M. S., and Moore, J. K.: Biogeochemical controls of surface ocean phosphate, Sci. Adv., 5, eaax0341, doi:10.1126/sciadv.aax0341, 2019.

McLennan, S. M.: Relationships between the trace element composition of sedimentary rocks and upper continental crust, Geochem. Geophy. Geosy., 2, doi:10.1029/2000gc000109, 2001.

Menzel Barraqueta, J. L., Klar, J. K., Gledhill, M., Schlosser, C., Shelley, R., Planquette, H. F., Wenzel, B., Sarthou, G., and Achterberg, E. P.: Atmospheric deposition fluxes over the Atlantic Ocean: A GEOTRACES case study, Biogeosciences, 16, 1525-1542, doi:10.5194/bg-16-1525-2019, 2019.

Middag, R., de Barr, H.J.W., and Bruland, K.W.: The relationships between dissolved zinc and major nutrients phosphate and silicate along the GEOTRACES GA02 transect in the western Atlantic Ocean, Global Biogeochem. Cy., 33, 63-84, doi.org/10.1029/2018GB006034, 2019.

Milne, A. C., Schlosser, C., Wake, B. D., Achterberg, E. P., Chance, R., Baker, A. R., Forryan, A., and Lohan, M. C.: Particulate phases are key in controlling dissolved iron concentrations in the (sub)tropical North Atlantic, Geophys. Res. Lett., 44, 2377-2387, doi:10.1002/2016GL072314, 2017.

Moore, C. M.: Diagnosing oceanic nutrient deficiency, Philisophical Transactions of the Royal Society A: Mathmatical, Physical and Engineering Sciences, 374, doi:10.1098/rsta.2015.0290, 2016.

Moore, C. M., Mills, M. M., Arrigo, K. R., Berman-Frank, I., Bopp, L., Boyd, P. W., Galbraith, E. D., Geider, R. J., Guieu, C., Jaccard, S. L., Jickells, T. D., La Roche, J., Lenton, T. M., Mahowald, N. M., Marañón, E., Marinov, I., Moore, J. K., Nakatsuka, T., Oschlies, A., Saito, M. A., Thingstad, T. F., Tsuda, A., and Ulloa, O.: Processes and patterns of oceanic nutrient limitation, Nat. Geosci., 6, 701-710, doi:10.1038/ngeo1765, 2013.

Moore, J. K., and Abbott, M. R.: Phytoplankton chlorophyll distributions and primary production in the Southern Ocean, J. Geophys. Res-Oceans, 105, 28709-28722, doi:10.1029/1999jc000043, 2000.

Morel, F. M. M.: The co-evolution of phytoplankton and trace element cycles in the oceans, Geobiology, 6, 318-324, doi:10.1111/j.1472-4669.2008.00144.x, 2008.

Morel, F. M. M., Reinfelder, J. R., Roberts, S. B., Chamberlain, C. P., Lee, J. G., and Yee, D.: Zinc and carbon co-limitation of marine-phytoplankton, Nature, 369, 740-742, doi:10.1038/369740a0, 1994.

Noble, A. E., Lamborg, C. H., Ohnemus, D. C., Lam, P. J., Goepfert, T. J., Measures, C. I., Frame, C. H., Casciotti, K. L., DiTullio, G. R., Jennings, J., and Saito, M. A.: Basin-scale inputs of cobalt, iron, and manganese from the benguela-angola front to the south atlantic ocean, Limnol Oceanogr, 57, 989-1010, doi.org/10.4319/lo.2012.57.4.0989, 2012.

Noble, A. E., Ohnemus, D. C., Hawco, N. J., Lam, P. J., and Saito, M. A.: Coastal sources, sinks and strong organic complexation of dissolved cobalt within the US North Atlantic GEOTRACES transect GA03, Biogeosciences, 14, 2715–2739, doi:10.5194/bg-14-2715-2017, 2017.

Nowicki, J. L., Johnson, K. S., Coale, K. H., Elrod, V. A., and Lieberman, S. H.: Determination of zinc in seawater using flow injection analysis with fluorometric detection, Anal. Chem, 66, 2732-2738, 10.1021/ac00089a021, 1994.

Ohnemus, D. C., and Lam, P. J.: Cycling of lithogenic marine particles in the US GEOTRACES North Atlantic transect, Deep-Sea Res. Pt II, 116, 283-302, doi:10.1016/j.dsr2.2014.11.019, 2015.

Ohnemus, D. C., Auro, M. E., Sherrell, R. M., Lagerstrom, M., Morton, P. L., Twining, B. S., Rauschenberg, S., and Lam, P. J.: Laboratory intercomparison of marine particle digestions including Piranha: A novel chemical method for dissolution of polyethersulfone filters, Limnol. Oceanogr-Meth., 12, 530-547, doi:10.4319/lom.2014.12.530, 2014.

Palter, J. B., Sarmiento, J. L., Gnanadesikan, A., Simeon, J., and Slater, R. D.: Fueling export production: nutrient return pathways from the deep ocean and their dependence on the Meridional Overturning Circulation, Biogeosciences, 7, 3549-3568, doi:10.5194/bg-7-3549-2010, 2010.

Paul, M., van de Flierdt, T., Rehkämper, M., Khondoker, R., Weiss, D., Lohan, M. C., and Homoky, W. B.: Tracing the Agulhas leakage with lead isotopes, Geophys. Res. Lett., 42, 8515-8521, doi:10.1002/2015gl065625, 2015.

Price, N. M., and Morel, F. M. M.: Cadmium and cobalt substitution for zinc in a marine diatom, Nature, 344, 658-660, doi:10.1038/344658a0, 1990.

Rapp, I., Schlosser, C., Rusiecka, D., Gledhill, M., and Achterberg, E. P.: Automated preconcentration of Fe, Zn, Cu, Ni, Cd, Pb, Co, and Mn in seawater with analysis using high-resolution sector field inductively-coupled plasma mass spectrometry, Anal. Chim. Acta, 976, 1-13, doi.org/10.1016/j.aca.2017.05.008, 2017.

Raux, E., Schubert, H. L., and Warren*, M. J.: Biosynthesis of cobalamin (vitamin B12): A bacterial conundrum, Cell. Mol. Life Sci., 57, 1880-1893, doi:10.1007/PL00000670, 2000.

Rodionov, D. A., Vitreschak, A. G., Mironov, A. A., and Gelfand, M. S.: Comparative genomics of the vitamin B12 metabolism and regulation in prokaryotes, J. Biol. Chem., 278, 41148-41159, doi:10.1074/jbc.M305837200, 2003.

Roshan, S., and Wu, J.: Cadmium regeneration within the North Atlantic, Global Biogeochem. Cy., 29, 2082-2094, doi.org/10.1002/2015GB005215, 2015.

Roshan, S., Wu, J., and Jenkins, W. J.: Long-range transport of hydrothermal dissolved Zn in the tropical South Pacific, Mar. Chem., 183, 25-32, doi.org/10.1016/j.marchem.2016.05.005, 2016.

Roshan, S., DeVries, T., Wu, J., and Chen, G.: The internal cycling of zinc in the ocean, Global Biogeochem. Cy., 32, 1833-1849, doi.org/10.1029/2018GB006045, 2018.

Saito, M. A., and Goepfert, T. J.: Zinc-cobalt colimitation of Phaeocystis antarctica, Limnol. Oceanogr., 53, 266-275, doi:10.4319/lo.2008.53.1.0266, 2008.

Saito, M. A., and Moffett, J. W.: Temporal and spatial variability of cobalt in the Atlantic Ocean, Geochim. Cosmochim. Ac., 66, 1943-1953, doi:10.1016/S0016-7037(02)00829-3, 2002.

Saito, M. A., Rocap, G., and Moffett, J. W.: Production of cobalt binding ligands in a Synechococcus feature at the Costa Rica upwelling dome, Limnol. Oceanogr., 50, 279-290, doi:10.4319/lo.2005.50.1.0279, 2005.

Saito, M. A., Moffett, J. W., Chisholm, S. W., and Waterbury, J. B.: Cobalt limitation and uptake in Prochlorococcus, Limnol. Oceanogr., 47, 1629-1636, doi:10.4319/lo.2002.47.6.1629, 2002.

Saito, M. A., Goepfert, T. J., Noble, A. E., Bertrand, E. M., Sedwick, P. N., and DiTullio, G. R.: A seasonal study of dissolved cobalt in the Ross Sea, Antarctica: Micronutrient behavior, absence of scavenging, and relationships with Zn, Cd, and P, Biogeosciences, 7, 4059-4082, doi:10.5194/bg-7-4059-2010, 2010.

Saito, M. A., Noble, A. E., Hawco, N., Twining, B. S., Ohnemus, D. C., John, S. G., Lam, P., Conway, T. M., Johnson, R., Moran, D., and McIlvin, M.: The acceleration of dissolved cobalt's ecological stoichiometry due to biological uptake, remineralization, and scavenging in the Atlantic Ocean, Biogeosciences, 14, 4637-4662, doi:10.5194/bg-14-4637-2017, 2017.

Sarmiento, J. L., Gruber, N., Brzezinski, M. A., and Dunne, J. P.: High-latitude controls of thermocline nutrients and low latitude biological productivity, Nature, 427, 56-60, doi:10.1038/Nature02127, 2004.

781 Schlitzer, R., Anderson, R. F., Dodas, E. M., Lohan, M., Geibert, W., Tagliabue, A., et al.: The
782 GEOTRACES intermediate data product 2017, Chemical Geology, 493, 210-223, 2018.

783 Shaked, Y., Xu, Y., Leblanc, K., and Morel, F. M. M.: Zinc availability and alkaline
784 phosphatase activity in Emiliania huxleyi: Implications for Zn-P co-limitation in the ocean,
785 Limnol. Oceanogr., 51, 299-309, doi:10.4319/lo.2006.51.1.0299, 2006.

786 Shelley, R. U., Zachhuber, B., Sedwick, P. N., Worsfold, P. J., and Lohan, M. C.:
787 Determination of total dissolved cobalt in uv-irradiated seawater using flow injection with
788 chemiluminescence detection, Limnol. Oceanogr-Meth., 8, 352-362,
789 https://doi.org/10.4319/lom.2010.8.352, 2010.

790 Sunda, W. G., and Huntsman, S. A.: Feedback interactions between zinc and phytoplankton in
791 seawater, Limnol. Oceanogr., 37, 25-40, doi:10.4319/lo.1992.37.1.0025 1992.

792 Sunda, W. G., and Huntsman, S. A.: Cobalt and zinc interreplacement in marine phytoplankton:
793 biological and geochemical implications, Limnol. Oceanogr., 40, 1404-1417,
794 doi:10.4319/lo.1995.40.8.1404, 1995.

795 Sunda, W. G., and Huntsman, S. A.: Control of Cd concentrations in a coastal diatom by
796 interactions among free ionic Cd, Zn, and Mn in seawater, Environ. Sci. Technol., 32, 2961-
797 2968, doi:10.1021/es980271y, 1998.

798 Sunda, W. G., and Huntsman, S. A.: Effect of Zn, Mn, and Fe on Cd accumulation in
799 phytoplankton: Implications for oceanic Cd cycling, Limnol. Oceanogr., 45, 1501-1516,
800 doi:10.4319/lo.2000.45.7.1501, 2000.

801 Tagliabue, A., Hawco, N. J., Bundy, R. M., Landing, W. M., Milne, A., Morton, P. L., and
802 Saito, M. A.: The role of external inputs and internal cycling in shaping the global ocean cobalt
803 distribution: insights from the first cobalt biogeochemical model, Global Biogeochem. Cy., 32,
804 594-616, doi:10.1002/2017gb005830, 2018.

805 Twining, B. S., and Baines, S. B.: The trace metal composition of marine phytoplankton, Annu.
806 Rev. Mar. Sci., 5, 191-215, doi:10.1146/annurev-marine-121211-172322, 2013.

807 Vance, D., Little, S. H., de Souza, G. F., Khatiwala, S., Lohan, M. C., and Middag, R.: Silicon
808 and zinc biogeochemical cycles coupled through the Southern Ocean, Nat. Geosci., 10, 202-
809 206, doi:10.1038/ngeo2890, 2017.

810 Weber, T., John, S., Tagliabue, A., and DeVries, T.: Biological uptake and reversible
811 scavenging of zinc in the global ocean, Science, 361, 72-76, doi:10.1126/science.aap8532,
812 2018.

813 Woodward, E. M. S., and Rees, A. P.: Nutrient distributions in an anticyclonic eddy in the
814 northeast Atlantic Ocean, with reference to nanomolar ammonium concentrations, Deep-Sea
815 Res. Pt II, 48, 775-793, doi:10.1016/S0967-0645(00)00097-7, 2001.

816 Worsfold, P. J., Achterberg, E. P., Birchill, A. J., Clough, R., Leito, I., Lohan, M. C., Milne,
817 A., and Ussher, S. J.: Estimating uncertainties in oceanographic trace element measurements,
818 Front. Mar. Sci., 5, doi10.3389/fmars.2018.00515, 2019.

819 Wu, J. F., Sunda, W., Boyle, E. A., and Karl, D. M.: Phosphate depletion in the western North
820 Atlantic Ocean, Science, 289, 759-762, doi:10.1126/science.289.5480.759, 2000.

821 Wyatt, N. J., Milne, A., Woodward, E. M. S., Rees, A. P., Browning, T. J., Bouman, H. A.,
822 Worsfold, P. J., and Lohan, M. C.: Biogeochemical cycling of dissolved zinc along the
823 GEOTRACES South Atlantic transect GA10 at 40°S, Global Biogeochem. Cy., 28, 44-56,
824 doi:10.1002/2013gb004637, 2014.

825 Xu, Y., Tang, D., Shaked, Y., and Morel, F. M. M.: Zinc, cadmium, and cobalt
826 interreplacement and relative use efficiencies in the coccolithophore Emiliania huxleyi,
827 Limnol. Oceanogr., 52, 2294-2305, doi:10.4319/lo.2007.52.5.2294, 2007.

828 Zubkov, M. V., Fuchs, B. M., Tarran, G. A., Burkill, P. H., and Amann, R.: High rate of uptake
829 of organic nitrogen compounds by Prochlorococcus cyanobacteria as a key to their dominance
830 in oligotrophic oceanic waters, Appl. Environ. Microb., 69, 1299–1304,
831 doi:10.1128/aem.69.2.1299-1304.2003, 2003.

832

833

834

835 Table 1. Analytical validation results for open ocean surface seawater (SAFe S), 1000 m
836 seawater (SAFe D2) and 2000 m seawater (GEOTRACES GD). All concentrations are in nM
837 (± 1 std. dev.). Consensus value conversion = 1.025 kg/L. ND indicates sample not determined.

838

	SAFe S	SAFe D2	GEOTRACES GD
Zn (FIA)	0.060 (0.020) *n* = 7	7.723 (0.091) *n* = 12	ND
Zn consensus value	0.071 (0.010)	7.616 (0.256)	1.753 (0.123)
Co (FIA)	0.004 (0.001) *n* = 3	0.049 (0.001) *n* = 2	0.073 (0.004) *n* = 5
Co consensus value	0.005 (0.001)	0.047 (0.003)	0.067 (0.001)

839

840

841 Table 2. Southeast Atlantic dissolved micro- and macronutrient mean concentration inventories
842 for the upper water column during early spring (D357-1), late spring (D357-2) and summer
843 (JC068) transects. STSW and SASW waters were defined using the θ 15°C isotherm (Section
844 3.4) and are compared with total inventories calculated for the shallower mixed layer (in
845 parenthesis) that include continental inputs of dissolved Zn and Co. Zn/PO_4^{3-}, Co/PO_4^{3-} and
846 Zn/Co represent the concentration inventory ratios for STSW and SASW, respectively. STSW
847 = Sub-Tropical Surface Water, SASW = Sub-Antarctic Surface Water.

848

Oceanographic Regime	Transect	Zn	Co	NO^{3-}	PO_4^{3-}	$Si(OH)_4$	Zn/PO_4^{3-}	Co/PO_4^{3-}	Zn/Co
		(nmol m^{-3})		(μmol m^{-3})			(μmol mol^{-1})		(mol mol^{-1})

STSW	Early spring	624 (1597)	32 (30)	2694 (870)	333 (203)	3735 (2790)	1876	97	19
	Late spring	384 (592)	23 (17)	1846 (763)	276 (191)	2781 (2326)	1387	82	17
	Summer	158 (139)	29 (24)	1557 (326)	226 (139)	2711 (1942)	699	129	5
SASW	Early spring	182 (112)	14 (13)	6035 (5300)	615 (566)	1875 (1847)	296	22	13
	Summer	83 (94)	12 (10)	4143 (3388)	439 (400)	1027 (886)	188	26	7

Figure 1. The Southeast Atlantic stations sampled for dissolved Zn and Co along the GA10 section during UK-GEOTRACES cruises D357 (red circles) and JC068 (black circles), overlain a VIIRS monthly composite image of chlorophyll-*a* concentrations for January 2012 (https://oceancolor.gsfc.nasa.gov/). Two transects were completed during D357 between Cape Town and the zero meridian that represent early austral spring 2010 (D357-1; Stns. 1, 2, 3, 4, 5 & 6) and late austral spring 2010 (D357-2; Stns. 0.5, 1, 1.5, 2.5, 3.5, 4.5), respectively. JC068 took place during austral summer 2011/12 and we present here only the repeat transect data between Cape Town and 13°W (Stns. 1, 2, 3, 7, 8, 9, 11). STSW = Sub-Tropical Surface Water, SASW = Sub-Antarctic Surface Water, AC = Agulhas Current, AR = Agulhas retroflection.

Figure 2. Upper 500 m potential temperature (θ) and dissolved PO_4^{3-} distributions for the Southeast Atlantic along early spring (a,b; D357-1), late spring (c,d; D357-2) and summer (e,f; JC068) transects. The dominant Southern Ocean (SASW & SAMW) and South Atlantic (STSW) water masses that influence the distribution of nutrients are shown. The θ 15°C isotherm (solid contour) represents a practical definition of the STF location, whilst SAMW is identified by the median potential density (σθ) isopycnal 26.8 kg m^{-3} (dashed contour, see Sect. 4.1.). STSW = Sub-Tropical Surface Water, SAMW = Sub-Antarctic Mode Water, AAIW = Antarctic Intermediate Water.

Figure 3. Upper 500 m dissolved Zn and Co distributions for the Southeast Atlantic along early spring (a,b; D357-1), late spring (c,d; D357-2) and summer (e,f; JC068) transects. The STF is delineated by θ 15°C (solid contour), whilst the influence of SAMW is evident by the median potential density (σθ) isopycnal 26.8 kg m^{-3} (dashed contour, see Section 4.1.). STSW = Sub-Tropical Surface Water, SAMW = Sub-Antarctic Mode Water, AAIW = Antarctic Intermediate Water. Note the changing y-axis scales for dZn distribution.

Figure 4. The dissolved Zn and Co versus PO_4^{3-} distribution for the Southeast Atlantic during early spring (a,b; D357-1), late spring (c,d; D357-2) and summer (e,f; JCO68) transects. The

green and red lines indicate the dZn:PO_4^{3-} regression slopes for SAMW and AAIW, respectively. The yellow line indicates the dCo:PO_4^{3-} regression slope for SAMW and AAIW combined. The equations for regression lines are detailed in Supplementary table 1. SAMW = Sub-Antarctic Mode Water, AAIW = Antarctic Intermediate Water. The full depth dZn:PO_4^{3-} relationship along JC068 can be found in Wyatt et al. (2014).

Figure 5. Seasonal differences in (a) pigment-derived taxonomic contributions to total chlorophyll-*a* (percentage), and (b) AFC counts of *Synechococcus*, *Prochlorococcus*, nanophytoplankton (approx. >2µm) and photosynthetic picoeukaryotes (approx. <2µm) in the Southeast Atlantic.

Figure 6. Metal/PO_4^{3-} inventory ratios for the upper water column of the Southeast Atlantic (horizontal bars) compared with laboratory estimates of cellular ratios in eukaryotic phytoplankton below which growth limitation occurs (solid vertical lines represent Zn:P with no added Co to media whilst dashed lines represent Co:P with no added Zn; phytoplankton data from Sunda and Hunstman, 1995). Error bars on inventory ratios represent 20 % combined uncertainty for dZn and dCo analyses (see Section 2.2). This figure is adapted from that in Saito et al. (2010) and implies that inter-seasonal differences in metal/PO_4^{3-} stoichiometry could impact phytoplankton community composition in the Southeast Atlantic.

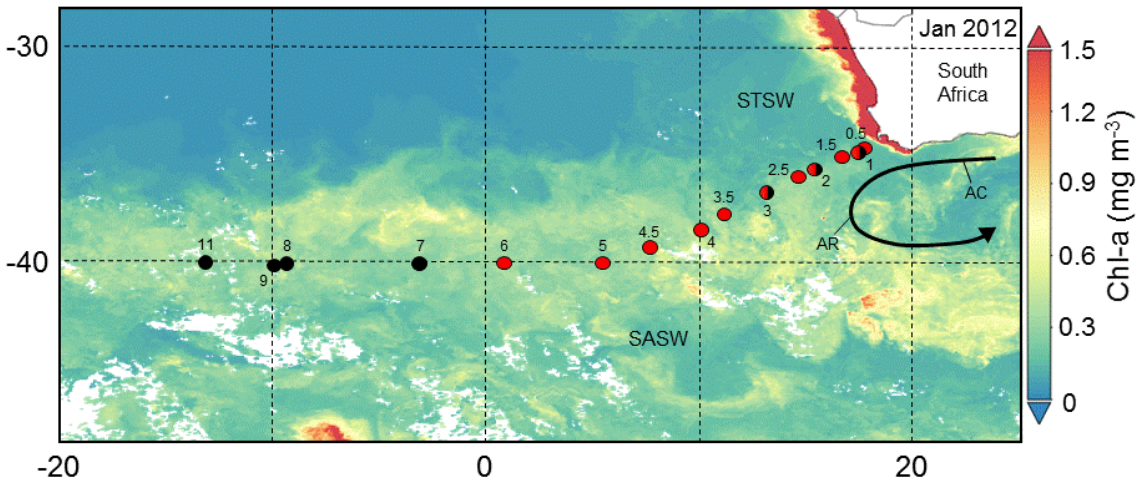

Figure 1.

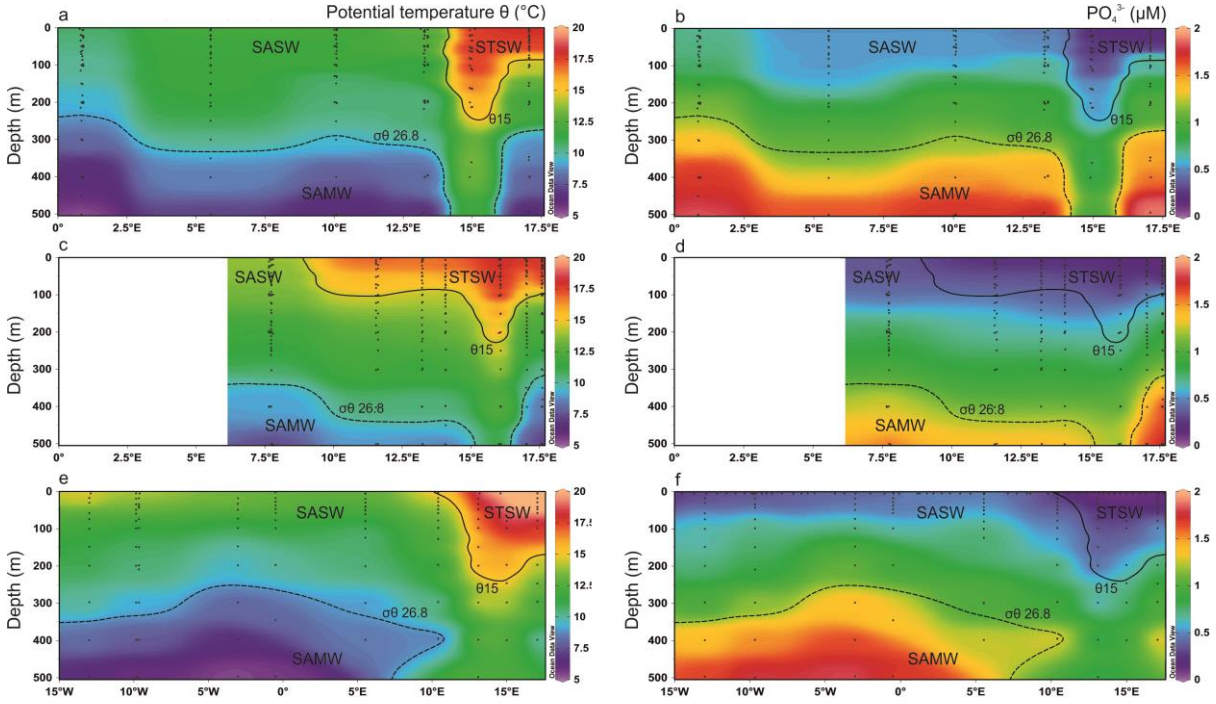

Figure 2.

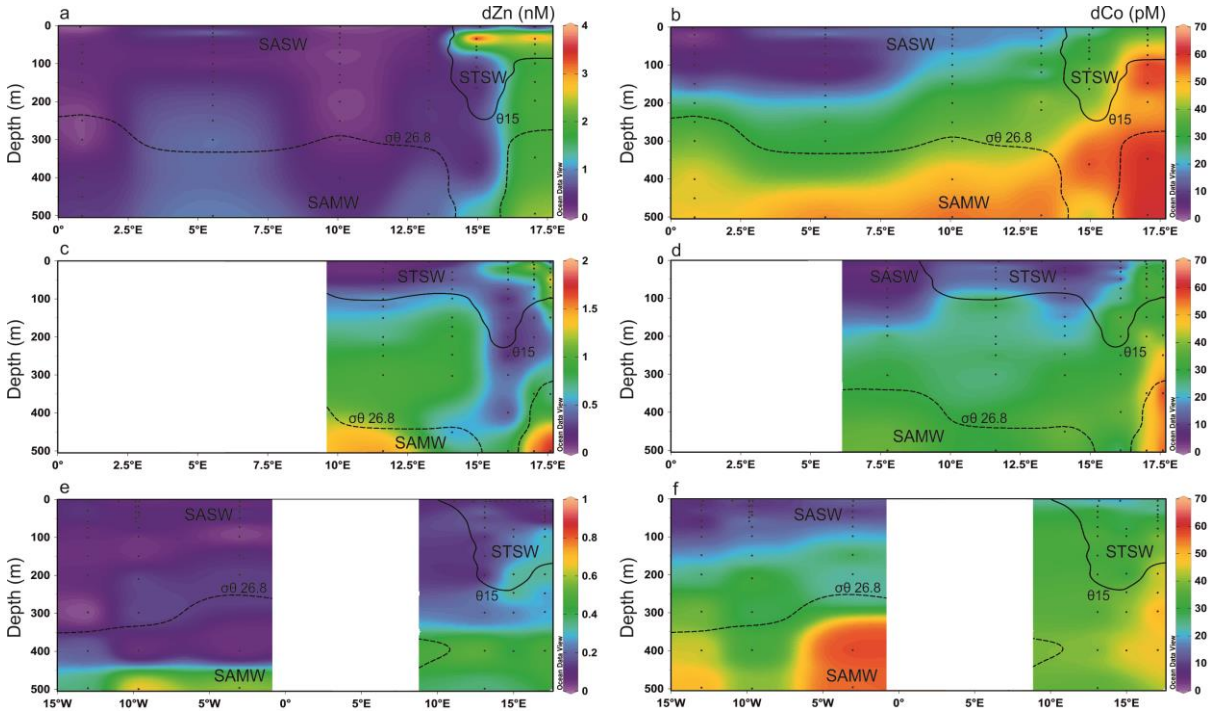

Figure 3.

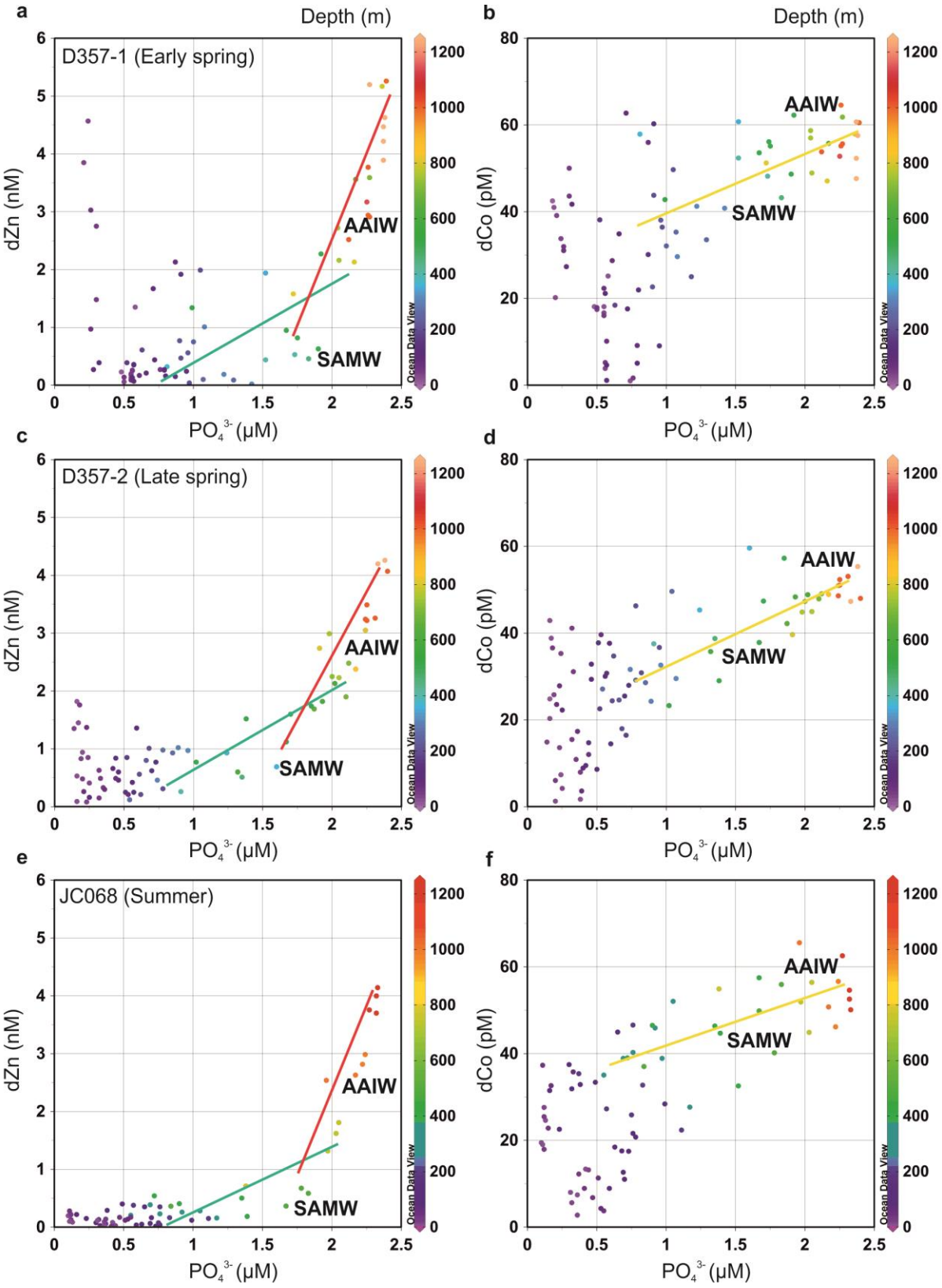
a
Depth (m)
D357-1 (Early spring)
dZn (nM)
AAIW
SAMW
PO_4^{3-} (μM)
Ocean Data View
b
Depth (m)
dCo (pM)
AAIW
SAMW
PO_4^{3-} (μM)
Ocean Data View
c
D357-2 (Late spring)
dZn (nM)
AAIW
SAMW
PO_4^{3-} (μM)
Ocean Data View
d
dCo (pM)
AAIW
SAMW
PO_4^{3-} (μM)
Ocean Data View
e
JC068 (Summer)
dZn (nM)
AAIW
SAMW
PO_4^{3-} (μM)
Ocean Data View
f
dCo (pM)
AAIW
SAMW
PO_4^{3-} (μM)
Ocean Data View

Figure 4.

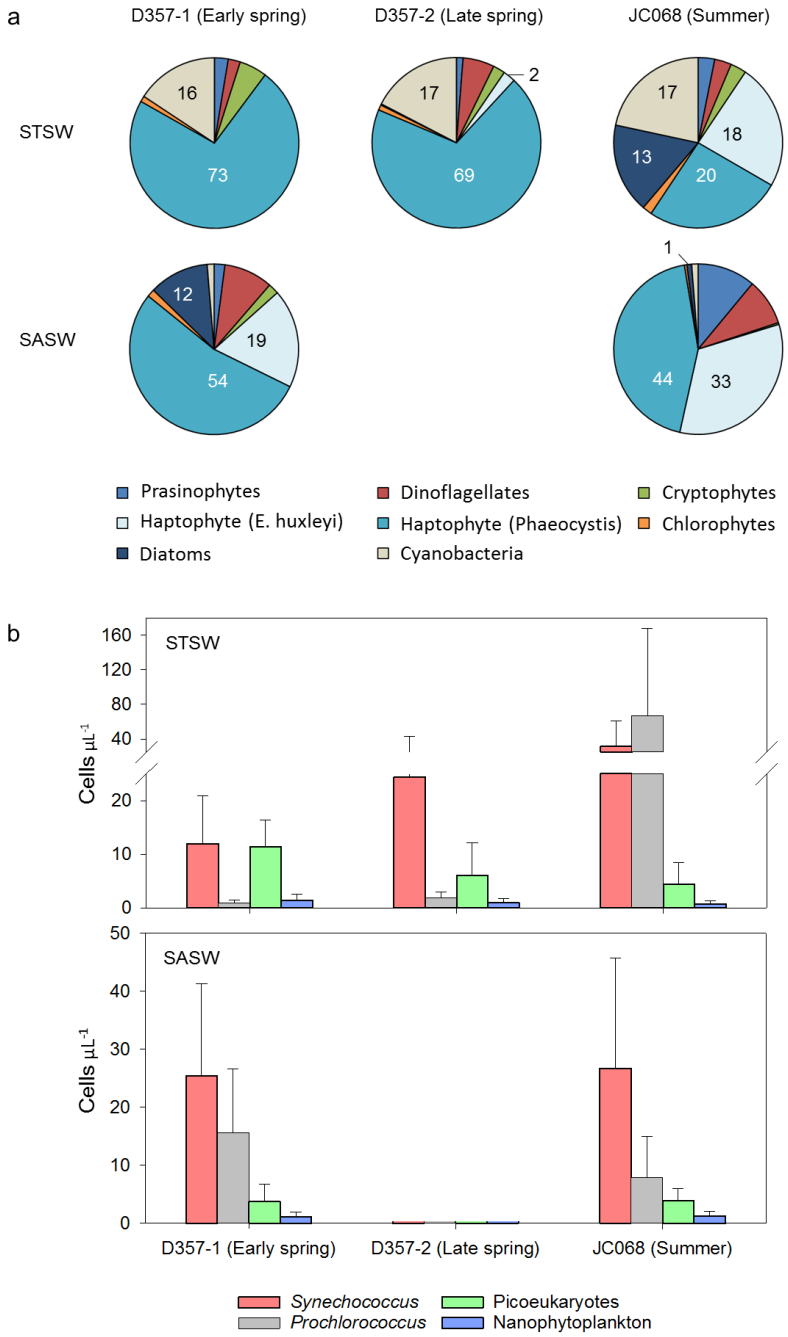

916

917 Figure 5.

918

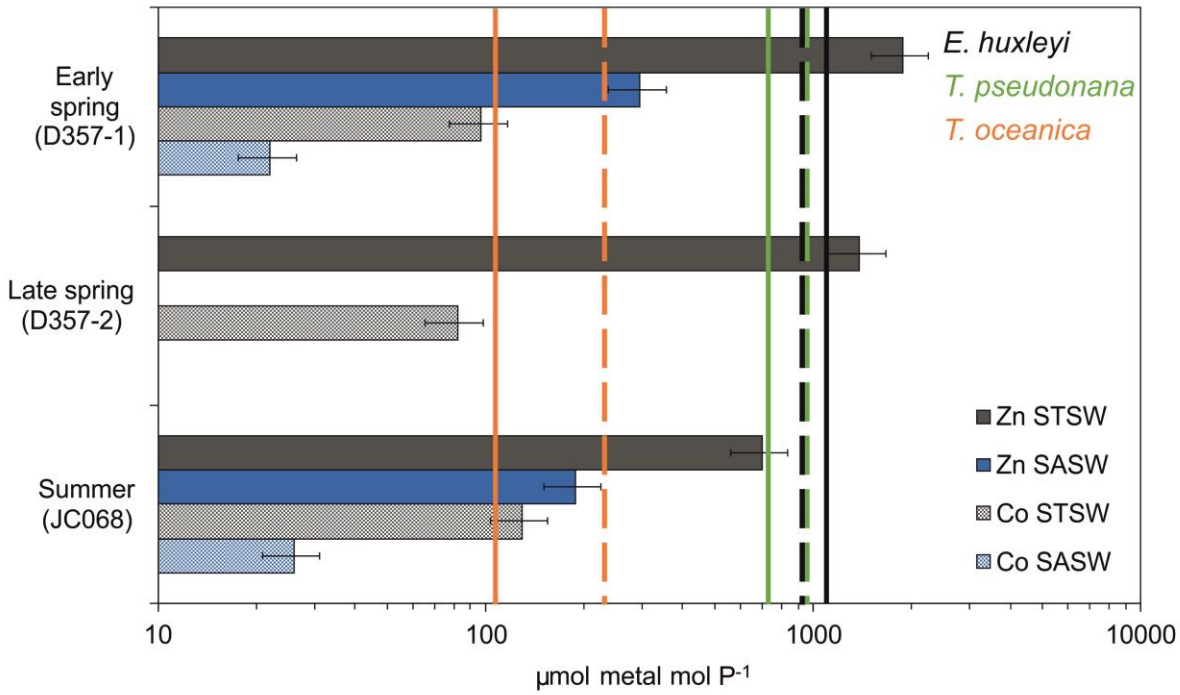
Early spring (D357-1)
Late spring (D357-2)
Summer (JC068)
E. huxleyi
T. pseudonana
T. oceanica
Zn STSW
Zn SASW
Co STSW
Co SASW
10
100
1000
10000
µmol metal mol P-1

Figure 6.